An adaptive capacity spectrum method for displacement-based seismic assessment of steel frames

M. Ferraioli, A. Lavino, A.M. Avossa & A. Mandara
Department of Civil Engineering, Second University of Naples

SUMMARY:
An adaptive version of the capacity spectrum method for displacement-based seismic assessment of steel frames is presented. The procedure can improve the efficiency of estimation of seismic demand and avoids the problems of no convergence and multiple solutions because it is non-iterative. Reliability of the procedure is verified by means of nonlinear dynamic analysis on structures subjected to earthquake records. The results are finally compared with the seismic response estimated with nonlinear static procedures proposed in FEMA 440-ATC-55.

Keywords: Steel frames, seismic performance assessment, adaptive pushover.

1. INTRODUCTION

A more rational approach for seismic evaluation of buildings should be based on inelastic displacement rather than elastic forces because structural damage is directly related to local deformations. As a consequence, there has been a growing interest in displacement-based seismic design (DBSD) and several articles on the subject can be found in literature. In this approach the displacement or interstorey drift is considered as the basic demand parameter in the design, evaluation and rehabilitation of structures. Estimating seismic demands at high performance levels, such as life safety and collapse prevention, requires explicit consideration of the inelastic behaviour of the structure. While nonlinear response history analysis (RHA) is the most rigorous procedure to estimate seismic demands, static pushover analysis are extensively employed to determine the deformation demands with acceptable accuracy without the intensive modelling and computational effort of RHA. The validity and applicability of these nonlinear static procedure have been extensively studied in literature. In particular, many researchers have compared the pushover curves with idealized envelopes obtained from incremental dynamic pushover analyses of structures subjected to artificial and natural input ground motions. The effectiveness of the Capacity Spectrum Method (CSM) has been validated by comparison with experimental results from pseudo-dynamic, cyclic and pushover tests. Various Nonlinear Static Procedures (NSPs) based on the CSM have been introduced in pre-standards reports and guidelines. Some of them were incorporated in the new generation of seismic codes to determine the deformation demand imposed on a building expected to behave inelastically. This study develops a simplified seismic demand estimation procedure in which the spectral characteristics of the ground motion are related to the inelastic deformation capacity for the structure.

2. CURRENT NONLINEAR STATIC PROCEDURES

Some Nonlinear Static Procedures (NSPs) proposed in literature were incorporated in the new generation of seismic codes to determine the deformation demand imposed on buildings expected to behave inelastically. In particular, ATC-40 Report (1997) proposes three nonlinear static procedures based on Capacity Spectrum Method (CSM). As an alternative, the Coefficient Method (CM) of FEMA-356 (2000) is based on a displacement modification procedure in which several empirically derived factors are used to modify the response of a linearly-elastic, single-degree-of-freedom model

of the structure. Both CM and CSM were found to provide substantially different estimates of target displacement for the same ground motion and the same building (Akkar & Metin, 2007; Chopra & Goel, 2000; Goel, 2007; Miranda & Luis-Garcia, 2002) and improved procedures have been proposed for estimating the target displacement.

2.1. Coefficient Method (FEMA-440)

To resolve the aforementioned inconsistencies, the recently released FEMA-440 document (ATC-55, 2003) reexamined the existing NSPs and proposed improvements to both procedures for displacement modification (CM) and procedures for equivalent linearization (CSM). In particular, the Coefficient Method of FEMA 356 has been modified using improved relationships for coefficients C_1 and C_2, and replacing the coefficient C_3 with a limitation on minimum strength to avoid dynamic instability due to strength degradation and P-Δ effects. The equivalent linearization procedures were modified with improved estimates of equivalent period and damping, and with an adjustment to generate a Modified Acceleration-Displacement Response Spectrum (MADRS) that does intersect the capacity spectrum at the Performance Point. In particular, the coefficients C_1 and C_2 are given by:

$$C_1 = \begin{cases} 1.0 + \dfrac{R-1}{0.04\,a} & T_e < 0.2\,s \\ 1.0 & T_e > 1.0s \\ 1.0 + \dfrac{R-1}{a\,T_e^2} & 0.2s < T_e < 1.0s \end{cases} \qquad C_2 = \begin{cases} 1.0 & T_e > 0.7s \\ 1.0 + \dfrac{1}{800}\left(\dfrac{R-1}{T_e}\right)^2 & T_e \le 0.7s \end{cases} \tag{2.1}$$

where a=130 for site class A and B, a=90 for site class C, a=60 for site classes D, E, and F. Finally, the coefficient C_3 is eliminated and substituted by a limitation on strength to avoid dynamic instability. This limitation on strength is specified by imposing a maximum limit on R given by:

$$R_{\max} = \frac{\Delta_d}{\Delta_y} + \frac{|\alpha_e|^{-h}}{4} \quad \text{with } h = 1.0 + 0.15\ln(T_e) \tag{2.2}$$

In Eqn. 2.2 Δ_d is the deformation corresponding to peak strength, Δ_y is the yield deformation, and α_e is the effective negative post-yield slope given by:

$$\alpha_e = \alpha_{P-\Delta} + \lambda(\alpha_2 - \alpha_{P-\Delta}) \tag{2.3}$$

where α_2 is the negative post-yield slope ratio; $\alpha_{P\text{-}\Delta}$ is the negative slope ratio caused by P-Δ effects; λ is the near-field effect given: λ=0.8 for $S_1 \ge 0.6$ and λ=0.2 for $S_1 < 0.6$ (S_1 is defined as the 1-second spectral acceleration for the Maximum Considered Earthquake). The α_2 slope includes P-Δ effects, in-cycle degradation, and cyclic degradation.

2.2. Capacity Spectrum Method (FEMA-440)

The improved FEMA-440 CSM includes new expressions to determine the effective period and effective damping developed by Guyader and Iwan (2006). Consistent with the original ATC-40 procedure, three iterative procedures for estimating the target displacement are also outlined. Finally, a limitation on the strength is imposed to avoid dynamic instability. Improved formulas for the effective period and viscous damping are proposed as a function of several coefficients tabulated in Table 6-1 and Table 6-2 of FEMA-440 document. The equivalent linearization procedures applied in practice normally require the use of spectral reduction factors to adjust an initial response spectrum to the appropriate level of effective damping β_{eff}. This factor $B(\beta_{eff})$ is a function of the effective damping and is used to adjust the spectral acceleration ordinates (defined for 5% damping) as follows:

$$(S_a)_\beta = (S_a)_{5\%} / B(\beta_{eff}) \tag{2.4}$$

where the damping coefficient $B(\beta_{eff})$ is given by:

$$B = \frac{4}{5.6 - \ln \beta_{eff}} \tag{2.5}$$

2.3. Adaptive modal combination procedures

Static pushover analysis is usually employed to determine the deformation demands with acceptable accuracy without the intensive modelling and computational effort of a dynamic analysis. The lateral force distribution should be defined to reproduce the inertia forces deriving from the earthquake ground motion. As the damage progresses, the inertia forces are redistributed, the vibration properties of the structure change and local plastic mechanism may occur. As a consequence, also the original participation and dynamic amplification of the mode shapes changes, and higher mode effects may be significantly increased. Therefore, multimodal and adaptive pushover analyses may be required to improve the accuracy of the deformation estimates. Several researchers have proposed adaptive force distributions that attempt to follow more closely the time-variant distributions of inertia forces. These approaches can give better estimations of the inelastic response, but they are conceptually complicated and computationally demanding for application in structural engineering practice. The Modal Pushover Analysis (MPA) (Chopra and Goel, 2002) allows for the change in load distribution due to damage of the structure without resorting to an adaptive load pattern. Target displacement values are computed by applying equivalent nonlinear procedures with a SDOF system representative of each modal load pattern and, finally, response quantities are combined with the SRSS method. Other authors (Antoniou and Pinho, 2004) proposed adaptive pushover procedures: Force-based adaptive pushover (FAP) and Displacement-based adaptive pushover (DAP). Particularly, in the force-based adaptive pushover approach (FAP), a modal analysis is performed step by step to update the force modal ratios. The lateral load distribution is continuously updated during the process according to modal properties, softening of the structure, its period elongation, and the modification of the inertial forces due to spectral amplification. The lateral load profiles of each vibration mode are then combined by using SRSS or CQC method. An incremental updating with increment of load calculated according to the spectrum scaling is applied at each analysis step. Despite its apparent conceptual superiority, the results obtained through FAP appear to be similar to those from conventional pushover analysis. Both types of analysis may give very poor prediction of deformation patterns. In the displacement-based adaptive pushover (DAP), the modal shape is directly imposed to the structure, using a displacement control analysis. The maximum interstorey drift values are obtained directly from modal analysis, rather than from the difference between not-necessarily simultaneous maximum floor displacement values. However, the use of SRSS or CQC rules to combine modal results lead to load vector shapes which neglect the possibility of sign change in storey displacements from different modes. Generally, the displacement-based adaptive pushover provides much improved approximation of highly irregular dynamic deformation profile envelopes, even if it assumes that all the interstorey drifts are maxima at the same time, which is of course not realistic. Two shortcomings of the modal combination rules can be pointed out: the first one is that the result obtained does not fulfil equilibrium; the second limitation is that signs are lost during the combination process eliminating the contribution of negative quantities. In other words, an “always-additive” inclusion of higher modes contribution is considered.

3. ADAPTIVE CAPACITY SPECTRUM METHOD

The conventional pushover analysis with invariant lateral force patterns may give inaccurate estimates of the deformation in case of local plastic mechanisms. This situation may occurs for both moment resisting frames (MRFs) and buckling restrained braced frames (BRBFs). For MRFs the traditional design provisions may be not effective to obtain a global plastic mechanism. In fact, the optimization of energy dissipation is pursued not directly through nonlinear response history analysis, but indirectly through design procedures essentially based on capacity design. For BRBFs the low post-yield stiffness provides minimal restoring force and thus drift can easily concentrate in one story. Therefore,

an adaptive pushover analyses is often required to improve the accuracy of nonlinear static procedure. In this study, the force-based adaptive pushover (FAP) is applied. This leads to variation both in lateral displacement pattern and in lateral force pattern. Therefore, also the equivalent SDOF system, which is representative of MDOF 3D model of the building in the CSM, changes during pushover analysis. In order to consider such effect, an adaptive version of the Capacity Spectrum Method (ACSM) is proposed. At each step of the pushover analysis a different equivalent SDOF system is defined as a function of the actual lateral displacement pattern. Particularly, the mass M_{eq} and the stiffness K_{eq} of the SDOF system in the ith step of pushover analysis is expressed as a function of the jth storey displacement δ_j^i and force F_j^i, as follows:

$$M_{eq}^i = \frac{\left(\sum_{j=1}^{N} m_j \cdot \delta_j^i\right)^2}{\sum_{j=1}^{N} m_j \cdot \delta_j^{i2}} \qquad K_{eq}^i = \frac{\left(\sum_{j=1}^{N} m_j \cdot \delta_j^i\right)^2}{\left(\sum_{j=1}^{N} m_j \cdot \delta_j^{i2}\right)^2} \sum_{j=1}^{N} F_j^i \cdot \delta_j^i \tag{3.1}$$

The transformation from Capacity Curve (V-δ_{TOP}) to Capacity Spectrum (S_a-S_d) in ADRS format (Acceleration-Displacement Response Spectra) is carried out step by step, as follows:

$$\Delta S_a^i = \Delta V^i \cdot \frac{\sum_{j=1}^{N} m_j \cdot \delta_j^{i2}}{\left(\sum_{j=1}^{N} m_j \cdot \delta_j^i\right)^2} \qquad \Delta S_d^i = \Delta \delta_{TOP}^i \frac{1}{\delta_N^i} \frac{\sum_{j=1}^{N} m_j \cdot \delta_j^{i2}}{\sum_{j=1}^{N} m_j \cdot \delta_j^i} \tag{3.2}$$

where ΔV^i and $\Delta \delta_{TOP}^i$ are the base shear increment and the corresponding roof displacement increment in the ith step of pushover analysis. Finally, a bilinear representation of the capacity spectrum (BCS) is developed such that the elastic stiffness is calculated at the base shear force corresponding to 60% of the yield base shear, and the area under the capacity spectrum and the bilinear representation is the same. Seismic demand is generally represented by means of Inelastic Demand Response Spectra (IDRS). In this paper the IDRS are indirectly computed scaling the 5% damped Elastic Demand Response Spectra (EDRS) by the strength reduction factor R_μ. In particular, the inelastic pseudo-acceleration S_a and displacement S_d, which are the coordinates of the IDRS in ADRS format, are characterized from the coordinates [S_{de} ; S_{ae}] of the EDRS (ξ=5%) as follows:

$$S_a = \frac{S_{ae}}{R_\mu} \qquad S_d = \frac{\mu \cdot S_{de}}{R_\mu} \tag{3.3}$$

where μ is the ductility ratio and R_μ is the ductility reduction factor defined by Vidic et el. (1994). R_μ depends from the ductility μ and, therefore, from the lateral displacement of the equivalent SDOF system. Consequently, an iterative procedure is usually required in order to estimate the intersection between IDRS and BCS. Applied for the displacement-based assessment the capacity spectrum method may become non-iterative. In fact, the performance-based assessment is displacement-based since the performance parameters used in the acceptance criteria are: plastic rotations, interstorey drifts and lateral displacement. As a consequence, the performance levels may be associated to the displacement demand of the structure. Then, the equivalence between MDOF and SDOF system gives the lateral displacement of the SDOF system at each performance level. Consequently, it can be fixed the position of the performance point (*PP*) on capacity spectrum in ADRS format (Fig. 3.1). This greatly simplifies the estimation of the intensity levels of the earthquake ground motion. In fact, the position of the *PP* gives the ductility ratio μ and ductility reduction factor R_μ without any iterative procedure. Consequently, the *PGA* may be increased until IDRS intersects BCS in *PP*, and the problems in convergence and accuracy of the iterative graphical procedures based on the Capacity Spectrum Method are avoided. The adaptive version of the Capacity Spectrum Method (ACSM) can be summarized in this sequence of steps:

1) Run the adaptive pushover analysis of the building.
2) Plot the Capacity Curve of the structure in terms of base shear V and roof displacement δ_{TOP}.
3) Define the equivalent SDOF system from Eqn. 3.1 and plot the CS in ADRS format using Eqn. 3.2.
4) Plot the EDRS (for ξ=5 per cent).
5) Define the bilinear representation of the capacity spectrum (BCS).
6) Calculate the lateral displacement of the SDOF system at each performance level using the acceptance criteria and plot the corresponding performance points (*PP*) on BCS.
7) Calculate the ductility ratio μ and the ductility reduction factor R_μ.
8) Define the Inelastic Demand Response Spectrum (IDRS) with scaling based on Eqn. 3.3.
9) Increase the PGA until IDRS intersects BCS in *PP*.

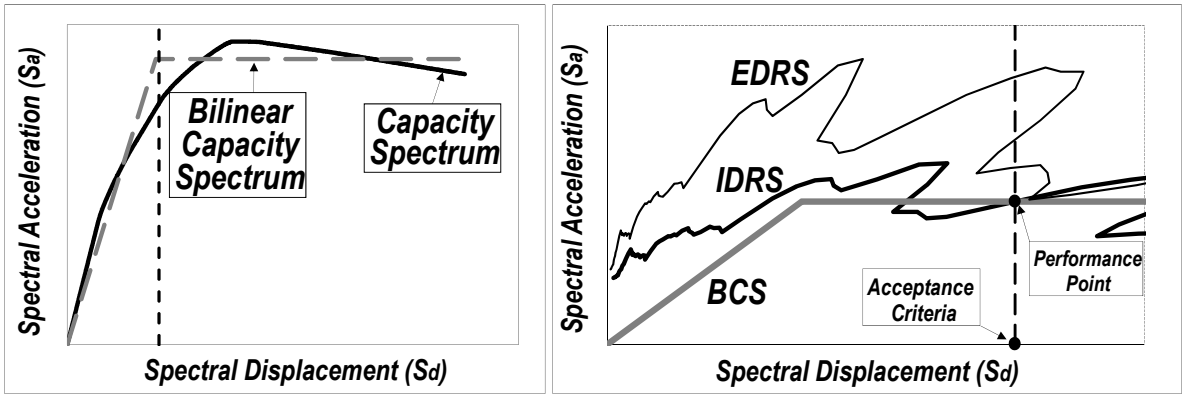

Figure 3.1. Bilinear representation of the capacity spectrum. Intersection between capacity and demand

4. VALIDATION AND COMPARISON WITH EXISTING METHODS

4.1. Study cases: Steel Moment Resisting Frames and Buckling Restrained Braced Frames

The adaptive capacity spectrum method (ACSM) is applied to both steel moment resisting frames (MRFs) and dual structural systems composed of steel frames and buckling-restrained braces (BRBFs). In particular, the following case studies are considered in the analyses: 1) 9-storey steel moment resisting frames designed according to Italian Code-NTC08 (2008); 2) 9-storey steel moment resisting frames designed with Plastic Design (Mazzolani et al., 1997); 3) 7-storey steel frame with buckling-restrained brace in the central span (Fig. 4.1). The interstorey height is 3.50 m for the first floor and 3.00 m for the other floors. The bay length is 5.00 m. Steel members are made from Italian S275 steel (f_y=275 MPa). For the moment resisting frames the design seismic action is defined considering soil class A, damping ratio ξ=5%, peak ground acceleration PGA=0.25g, behaviour factor q=6.5. The design sections of the two steel frames are reported in Tab. 4.1. For the 7-storey dual structural system the steel frame was designed to resist dead loads according to the allowable stress design method. The design sections of the steel frame are reported in Tab. 4.2. The cross-sectional area of buckling-restrained braced frames was defined as a function of the story stiffness ratio (S_R) between the lateral stiffness K_b of the brace and the lateral stiffness K_F of the main frame. In particular, the following values are considered: a) S_R =5; b) S_R =10; c) S_R =15. The lateral stiffness of BRB is $K_b = S_R K_F$ and thus the required cross-sectional is:

$$A_b = \frac{S_R \cdot K_F \cdot L_b}{E_b \cdot \cos^2 \theta} \tag{4.1}$$

where L_b, E_b and θ are, respectively, the length, the elastic modulus and the slope of the brace. The story-wise distribution of BRB was selected with the following three methods: BRB1) cross-sections distributed proportional to story stiffness; BRB2) same cross-section used in first story; BRB3) the cross-sections of BRBs are designed in order to have simultaneous yielding. The modal properties of the MRFs and BRBFs are reported in Tabs. 4.3-4.4.

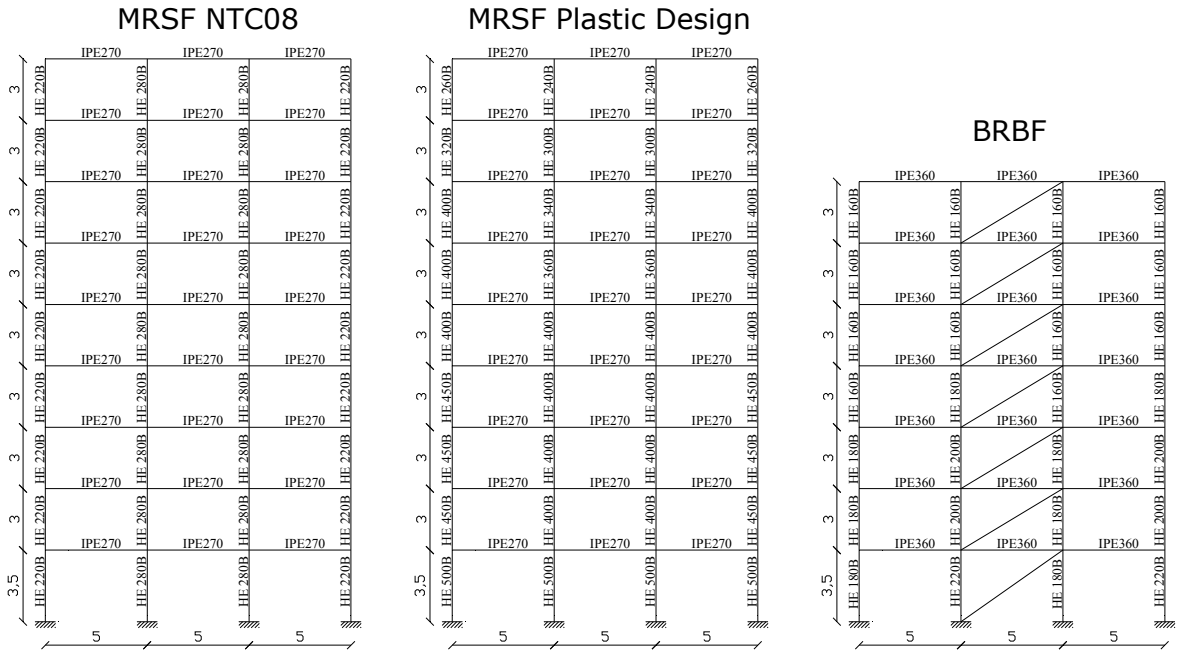

Figure 4.1. Study cases: moment resisting frames and buckling-restrained frame.

Table 4.1. Design sections of steel moment resisting frames

N.	9 Storeys 3 Bays – Italian Code 2008 (NTC08)			9 Storeys 3 Bays – Plastic Design (PD)		
	Beams	External Columns	Internal Columns	Beams	External Columns	Internal Columns
1	IPE270	HE220B	HE280B	IPE270	HE500B	HE500B
2	IPE270	HE220B	HE280B	IPE270	HE450B	HE400B
3	IPE270	HE220B	HE280B	IPE270	HE450B	HE400B
4	IPE270	HE220B	HE280B	IPE270	HE450B	HE400B
5	IPE270	HE220B	HE280B	IPE270	HE400B	HE400B
6	IPE270	HE220B	HE280B	IPE270	HE400B	HE360B
7	IPE270	HE220B	HE280B	IPE270	HE400B	HE340B
8	IPE270	HE220B	HE280B	IPE270	HE320B	HE300B
9	IPE270	HE220B	HE280B	IPE270	HE260B	HE240B

Table 4.2. Design Sections of buckling-restrained braced frames.

N.	Beams	External Columns	Internal Columns	N.	Beams	External Columns	Internal Columns
1	IPE360	HE180B	HE220B	5	IPE360	HE160B	HE160B
2	IPE360	HE180B	HE200B	6	IPE360	HE160B	HE160B
3	IPE360	HE180B	HE200B	7	IPE360	HE160B	HE160B
4	IPE360	HE160B	HE180B				

Table 4.3. Fundamental periods and modal mass ratios. Buckling-restrained braced frames

	First mode		Second mode		Third mode	
	T(s)	α(%)	T(s)	α(%)	T(s)	α(%)
BRB1 - S_R=5	1.11	79.8	0.39	13.65	0.23	3.25
BRB2 - S_R=5	1.06	82.0	0.36	12.56	0.20	3.13
BRB3 - S_R=5	1.13	78.0	0.44	12.44	0.28	4.76
BRB1 - S_R=10	0.95	77.7	0.32	15.14	0.18	3.50
BRB2 - S_R=10	0.91	79.4	0.30	14.50	0.16	3.48
BRB3 - S_R=10	0.96	75.9	0.37	12.58	0.23	5.67
BRB1 - S_R=15	0.87	76.3	0.28	16.07	0.16	3.69
BRB2 - S_R=15	0.84	77.6	0.27	15.68	0.15	0.22
BRB3 - S_R=15	0.89	74.7	0.33	13.53	0.21	5.84

Table 4.4. Fundamental periods and modal mass ratios. Steel moment resisting frames

	First mode		Second mode		Third mode	
	T(s)	α(%)	T(s)	α(%)	T(s)	α(%)
Italian Code NTC08	2.57	82	0.82	10	0.45	0.30
Plastic Design	2.11	75	0.64	11	0.33	0.50

4.2. Numerical modelling and analysis methods

A distributed plasticity fiber element model implemented in Seismostruct (2011) is considered in the analyses. Sources of geometrical nonlinearity considered are both local and global. The spread of plasticity along the element derives from an inelastic cubic formulation with two Gauss points to use for numerical integration of the equilibrium equations. A bilinear model with kinematic strain-hardening of 0.5% is used for steel. Component test results showed that BRBFs can have very high ductility and cumulative ductility capacities without any degradation in their strength and stiffness (Fahnestock, 2007). As a consequence, also considering very conservative ductility values (maximum ductility of 15; cumulative ductility capacity of 200) the structural limit states are conditioned by the performance levels of the main frames. Thus, the structural performance levels defined for steel frames in FEMA 356 (Tab. C1.3) are considered in the analysis. In particular, the acceptance criteria are based on the following performance parameters: 1) transient drift=0.7% for Immediate Occupancy (IO); 2) transient drift=2.5% for Life Safety (LS); 3) transient drift=5% for Collapse Prevention (CP).
The adaptive version of the capacity spectrum method here proposed is compared con the following current nonlinear static procedures: 1) FEMA 440 Coefficient Method (CM); 2) FEMA 440 Capacity Spectrum Method (CSM). In order to verify the accuracy of nonlinear static procedures and the sensitivity to input ground motion, these NSPs are compared with the predictions of nonlinear dynamic analysis. In particularly, a set of input ground motions is selected to be consistent to 5%-damped EC8 elastic spectrum for soil class A. In Fig. 4.2 the envelope values of the spectral acceleration are compared to EC8 elastic response spectra. In Figs. 4.3-4.6 the peak ground acceleration (*PGA*) of the input ground motion is correlated to the corresponding total drift ratio (roof displacement/height). The results are obtained with nonlinear static procedures (NSPs) and Incremental Nonlinear Dynamic Analysis (IDA). In particular, the figures show the performance points obtained using various nonlinear static procedures (ACSM, FEMA-440 CSM, FEMA-440 CM) for the three limit states: Immediate Occupancy (IO), Life Safety (LS), Collapse Prevention (CP). The IDA consists in performing a series of nonlinear time-history analysis, using an acceleration input ground motion scaled to increasing amplitudes. Each IDA point in the graph is defined from the maximum total drift (maximum displacement/height) during dynamic analysis and the corresponding peak ground acceleration. Of course, the peak ground acceleration representing the actual capacity of the structure depends on the earthquake input ground motion. Thus, in order to evaluate the dispersion characteristics the figures show the mean value and the mean ± standard deviation value of the data set for static analyses and the mean + standard deviation value for dynamic analyses. The mean is reported as the measure of central tendency and the standard deviation as the measure of dispersion.

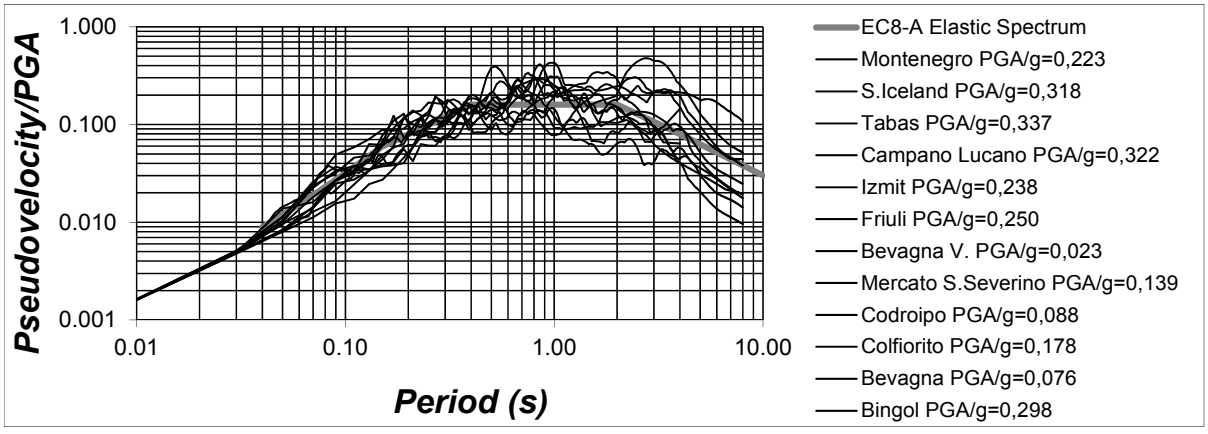

Figure 4.2. Ground motion response spectra and Eurocode 8 elastic response spectrum

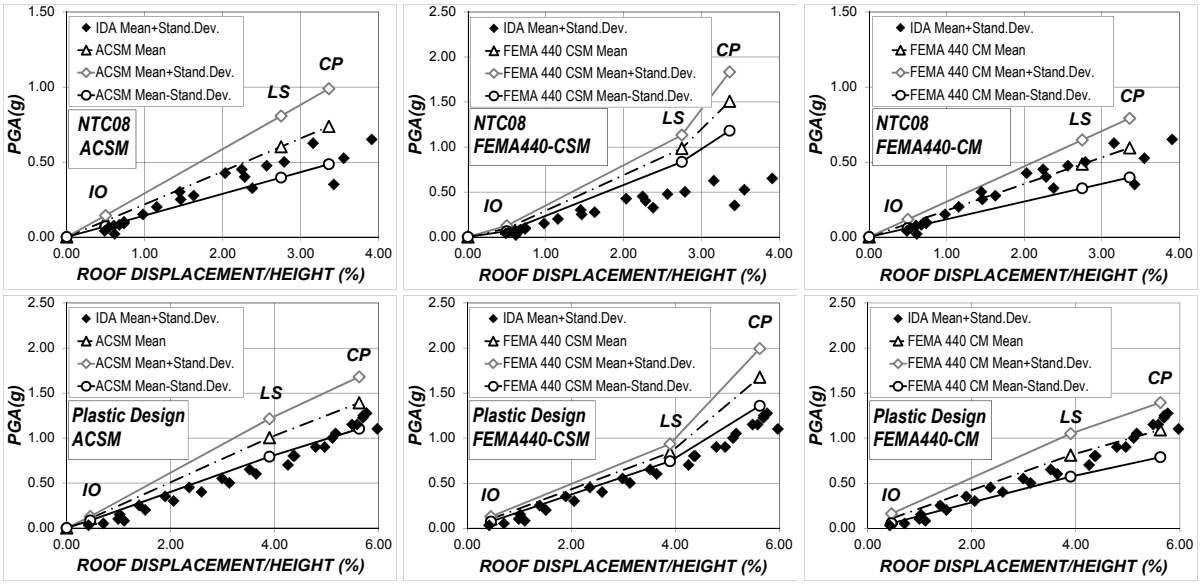

Figure 4.3. Peak ground acceleration versus roof displacement. NSP and Incremental Dynamic Analysis. Moment Resisting Steel Frames (MRSF).

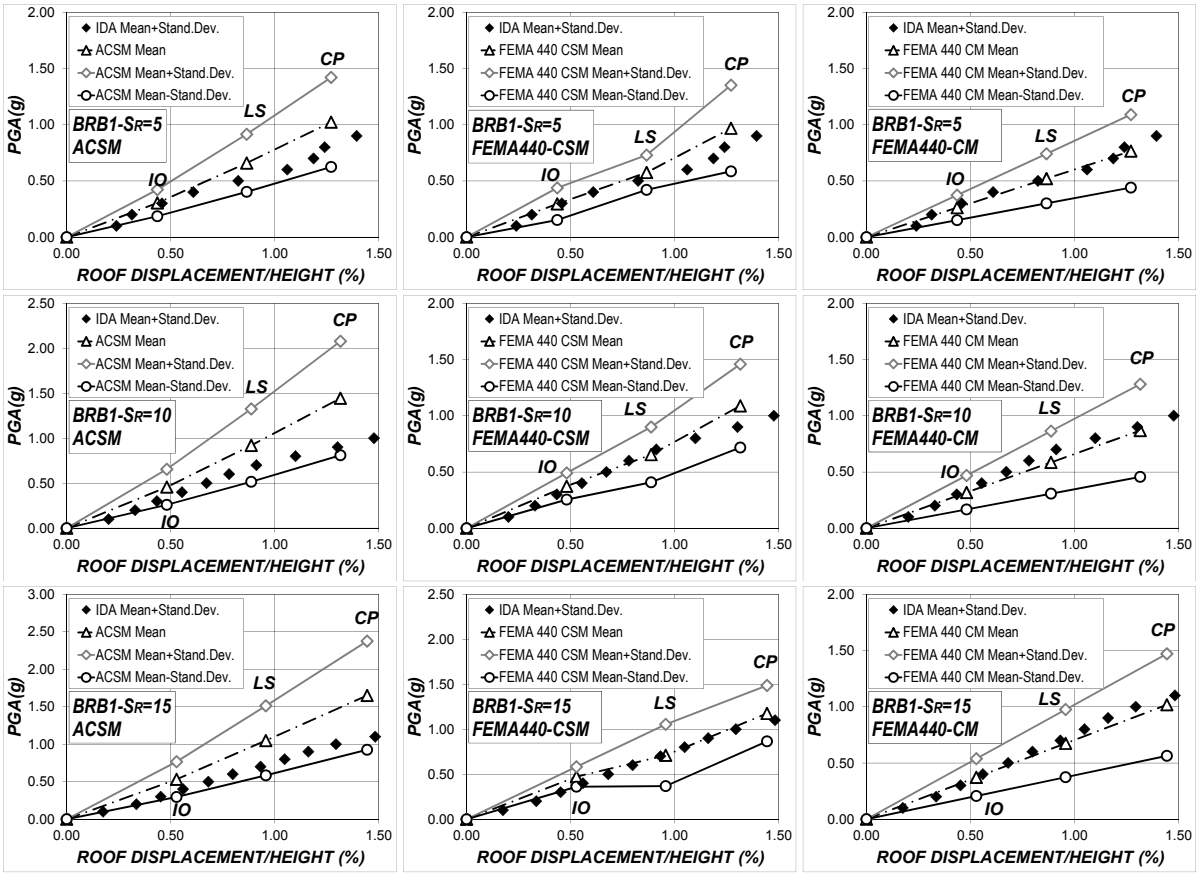

Figure 4.4. Peak ground acceleration versus roof displacement. NSP and Incremental Dynamic Analysis. Buckling Restrained Braced Frames (BRB1 Structure)

The comparison between the mean-standard deviation plot from nonlinear static analysis and the mean+standard deviation plot from nonlinear response history analysis gives a measure of the reliability of NSPs. The results obtained show that the ACSM generally gives the better estimation of the seismic performance of the structure obtained from RHA. The smaller dispersion is obtained with FEMA-440 CSM procedure.

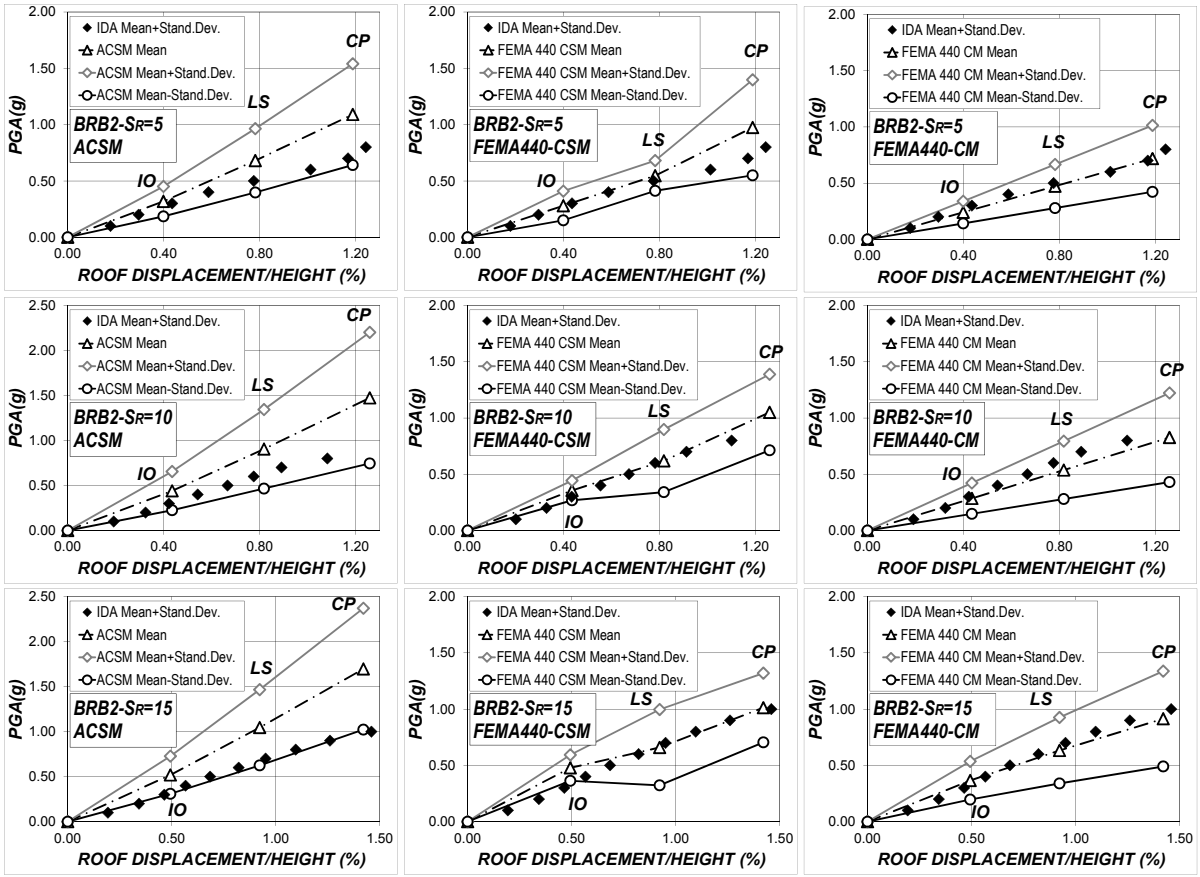

Figure 4.5. Peak ground acceleration versus roof displacement. NSP and Incremental Dynamic Analysis. Buckling Restrained Braced Frames (BRB2 Structure)

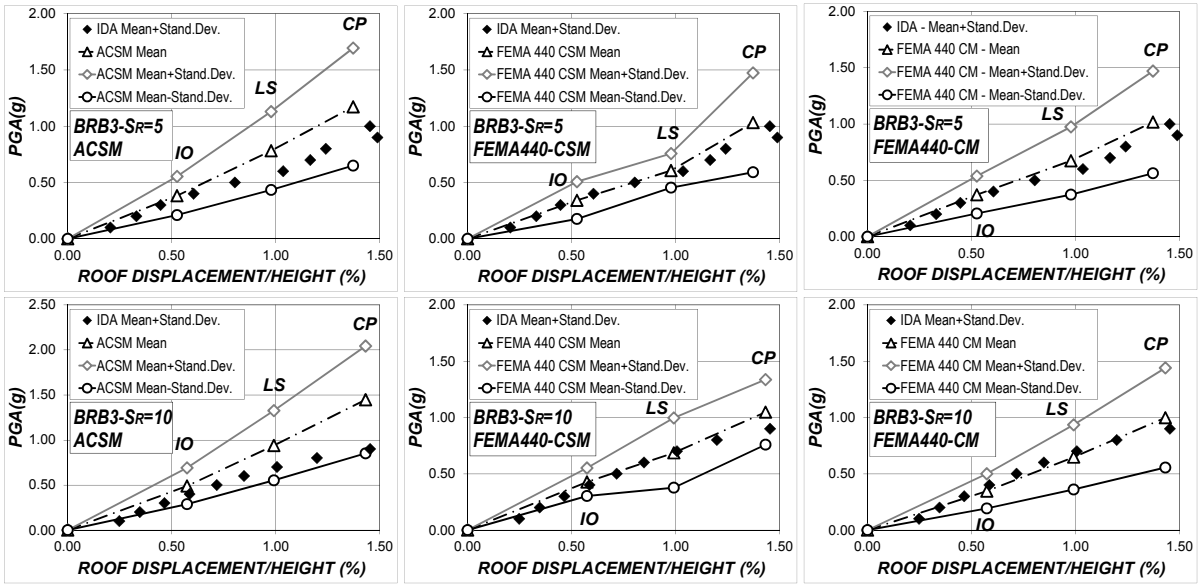

Figure 4.6. Peak ground acceleration versus roof displacement. NSP and Incremental Dynamic Analysis. Buckling Restrained Braced Frames (BRB3 Structure)

In the case of MRSFs designed with NTC08 the procedure FEMA440-CSM may be not conservative with respect to incremental nonlinear dynamic analysis, because it tends to underestimate the total drift. On the contrary, for the MRSFs designed with Plastic Design all the considered NSPs seem to give an accurate estimation of inelastic dynamic response. In the case of BRBFs all the NSPs here considered give conservative assessment of the seismic performance of the structure.

5. CONCLUSIONS

An adaptive capacity spectrum method (ACSM) for displacement-based seismic assessment of steel frames is proposed. The method incorporates adaptive pushover, capacity spectrum method and inelastic demand spectra. The accuracy in predicting the seismic-induced demands of the steel structures is investigated by comparison with results from FEMA-440 procedures and from Incremental Dynamic Analysis (IDA), using response spectrum compatible earthquake ground motions. Steel moment resisting frames and buckling restrained braced frames with different lateral stiffness and story-wise distribution of braces are considered in the analyses. Comparison of FEMA-440 procedures, adaptive capacity spectrum method and time-history analyses show the efficiency of ACSM that better reproduce results of incremental dynamic analysis with respect to conventional procedures that may give not conservative assessments of seismic response.

REFERENCES

AISC/SEAOC. (2001). Recommended Provisions for BRB, Structural Engineers Association of California: Seismology and Structural Standards Committee and American Institute of Steel Construction, Inc.

Akkar, S. and Metin, A. (2007). Assessment of Improved Nonlinear Static Procedures in FEMA-440. *Journal of Structural Engineering* **133(9)**: 1237-1246.

Antoniou, S. and Pinho, R. (2004). Advantages and Limitations of Adaptive and Non-Adaptive Force-Based Pushover Procedures *Journal of Earthquake Engineering* **8:4**. 497–522.

ASCE/SEI 7-05. (2005). Minimum Design Loads for Buildings and Other Structures.

ATC-40. (1997). Seismic Evaluation and Retrofit of Concrete Buildings. Report No. ATC-40, Applied Technology Council, Redwood City, CA.

Chopra, A.K. and Goel, R.K. (2000). Evaluation of NSP to Estimate Seismic Deformation: SDF Systems. *Journal of Structural Engineering* **126(4)**: 482-490.

D'Aniello, M., Della Corte, G., Mazzolani, F.M. and Landolfo, R. (2006). Steel Buckling Restrained Braces. In: *Seismic upgrading of RC buildings by advanced techniques - The ILVA-IDEM Research Project*. Polimetrica Publisher, Italy. 179-223.

Dipti. R. and Sahoo, Shih-Ho Chao. (2010). Performance-based plastic design method for buckling-restrained braced frames. *Engineering Structures* **32**: 2950-2958.

Fahnestock, LA, Ricles, J.M. and Sause, R. (2007). Experimental evaluation of a large-scale buckling-restrained braced frame. *Journal Structural Engineering* **133(9)**: 1205-14.

FEMA 440 (2005). *Improvement of nonlinear static seismic analysis procedures*, prepared by the Applied Technology Council (ATC-55 Project), published by the Federal Emergency Management Agency, Washington.

FEMA 356 (2000). *Prestandard and Commentary for the Seismic Rehabilitation of Buildings*, prepared by the American Society of Civil Engineers for the Federal Emergency Management Agency. Washington, D.C.

Ferraioli, M., Lavino, A., Avossa, A.M. and Mandara, A. (2008). Displacement-based seismic assessment of steel moment resisting frame structures. *14th World Conference on Earthquake Engineering*. October 12-17. Beijing, China.

Goel, R.K. and Chadwell, C. (2007). *Evaluation of Current Nonlinear Static Procedures for Concrete Buildings Using Recorded Strong-Motion Data*, Final Report, California Strong Motion Instrumentation Program, Sacramento, CA.

Guyader, A.C. and Iwan, W.D. (2006). Determining Equivalent Linear Parameters for Use in a Capacity Spectrum Method. *Journal of Structural Engineering* **132(1)**: 59-67.

Italian Code NTC08, D.M. 14.01.08, G.U. No.9 – 04.02.08 (in Italian), (2008).

Kim, J. and Choi, H. (2004). Behavior andd esign of structures with buckling-restrained braces. *Engineering Structures* **26**: 693–706.

Miranda, E. and Ruiz-Garcia, J. (2002). Evaluation of Approximate Methods to Estimate Maximum Inelastic Displacement Demands. *Earthquake Engineering and Structural Dynamics* **31(3)**: 539-560.

Ragni, L., Zona, A. and Dall'Asta, A. (2011). Analytical expressions for preliminary design of dissipative bracing systems in steel frames, *Journal of Constructional Steel Research* **67**: 102-113.

Sabelli, R., Mahin, S. and Chang, C. (2003). Seismic demands on steel braced frame buildings with buckling restrained braces. Engineering Structures **25**, 655–666.

SeismoSoft (2011). SeismoStruct. A computer program for static and dynamic analysis for framed structures. (online) available from URL: www.seismosoft.com.

Vidic, T., Fajfar, P. and Fischinger, M. (1994). Consistent inelastic design spectra: strength and displacement. *Earthquake Engineering and Structural Dynamics* **23**: 502-521.